Signal Processing 89 (2009) 913–920

Contents lists available at ScienceDirect

Signal Processing

journal homepage: www.elsevier.com/locate/sigpro

Off-broadside main beam design and subband implementation for a class of frequency invariant beamformers

Wei Liu [a,*], Stephan Weiss [b]

[a] Communications Research Group, Department of Electronic and Electrical Engineering, University of Sheffield, UK
[b] Centre for excellence in Signal & Image Processing, Department of Electronic and Electrical Engineering, University of Strathclyde, Glasgow, UK

ARTICLE INFO

Article history:
Received 10 July 2008
Received in revised form
4 November 2008
Accepted 14 November 2008
Available online 24 November 2008

Keywords:
Frequency invariant beamforming
Broadband arrays
Filter banks
Subband beamforming
Scaled aperture

ABSTRACT

The design of frequency invariant beamformers (FIBs) with off-broadside main beams is studied and it is shown that the required FIR filter length in this case should be much larger than the one with a broadside main beam. To reduce the computational complexity of such a beamformer and also improve its frequency invariant property at lower frequencies, two subband implementations are proposed. In the first one, the fullband array signals are split into subbands by a bank of analysis filters and the corresponding decimated subband signals form a series of subband arrays. Based on this standard subband structure, we then change the sensor spacings of different subband signals so that lower frequency bands have a larger spacing, which leads to a class of FIBs with scaled aperture with further improved performance at lower frequencies.

1. Introduction

In the past, beamforming has been studied extensively due to their wide applications to sonar, radar and communications [1]. Amongst them is a class of broadband beamformers with frequency invariant beam patterns, which can form beams pointing to the signal of interest with a constant beamwidth. One of the suggested methods is to optimise the array parameters with respect to the desired response using available convex optimisation methods [2–5]. A systematic method was proposed in [6], which can be applied to one-dimensional (1-D), two-dimensional (2-D) and three-dimensional (3-D) arrays, where each array element is followed by its own primary filter and the outputs of these primary filters share a common secondary filter to form the final output. However, beyond the 1-D array case this design method can be very complicated.

Most recently, a new class of frequency invariant arrays exploiting the Fourier transform relationship between the array's spatial and temporal parameters and its beam pattern was proposed [7–9], where the design can be achieved based on a simple multi-dimensional inverse Fourier transform. However, it has been found that with the same number of array sensors and array coefficients, the off-broadside main beam design is not as good as the broadside main beam in terms of its frequency invariance property.

In this work we will study this problem in detail and show that an increase of the temporal dimension of the beamformer in combination with a denser sampling grid in the Fourier domain can achieve a better result. However, the increase of the temporal dimension leads to a much higher computational complexity in implementation. In the past, in order to reduce the computational complexity and improve the performance of the system, subband methods have been proposed for broadband adaptive beamforming [10–13] and here we propose to implement the frequency invariant beamformer (FIB) in subbands too.

* Corresponding author.
E-mail addresses: w.liu@sheffield.ac.uk (W. Liu), stephan.weiss@eee.strath.ac.uk (S. Weiss).

0165-1684/$ - see front matter © 2008 Elsevier B.V. All rights reserved.
doi:10.1016/j.sigpro.2008.11.010

Two subband implementations will be proposed and in the first one, each received array signal is split into K decimated subbands by an analysis filter bank and the corresponding subband signals form K sets of subband arrays and an FIB is operated in each of the subband arrays. The outputs of the subband FIBs are then combined together by a synthesis filter bank to form the fullband output signal. When the required spatio-temporal dimension of the fullband array becomes large enough, the subband implementation will have a much lower computational complexity. As the spatio-temporal distribution of the subband signals at each of the subband arrays is different from the original fullband signal, we cannot use the design method for fullband arrays directly. Therefore, a modified method for the subband FIB design is proposed. In a refinement, we modify this subband FIB structure for use with nested arrays.

This paper is organised as follows. A review of the FIB design for linear arrays will be given in Section 2. In Section 3, the problem for off-broadside main beam design will be discussed in detail, followed by the proposed solution. We then study the two subband implementations in Section 4 with design examples provided for each case. Conclusions are drawn in Section 5.

2. Frequency invariant beamforming

Although the method proposed in [8,9] can be applied to 1-D, 2-D and 3-D broadband arrays, without loss of generality, we here focus on the 1-D case and only consider the uniform linear array.

A uniform linear array with a sensor spacing of d_x is shown in Fig. 1. The received signal by the m-th sensor is sampled with a sampling period of T and then processed by an FIR filter with coefficients $d[m,n]$, $m=0,\ldots,M-1$, $n=0,\ldots,J-1$. We take the first sensor as the zero phase reference point for the impinging signals. Then the array's response can be written as

$$R(\Omega,\theta)=\sum_{m=0}^{M-1}\sum_{n=0}^{J-1} d[m,n]\mathrm{e}^{-\mathrm{j}m\mu\Omega\sin\theta}\mathrm{e}^{-\mathrm{j}n\Omega}, \tag{1}$$

where $\mu=d_x/cT$, $\Omega=\omega T$ is the normalised angular frequency and c the wave propagation speed. To avoid aliasing in both the spatial and temporal domains, we can choose $d_x=\lambda_{\min}/2$ and $T=\lambda_{\min/2c}$, where $\lambda_{\min}$ is the wavelength corresponding to the maximum frequency of interest. As a result, we have $\mu=1$. With the substitutions

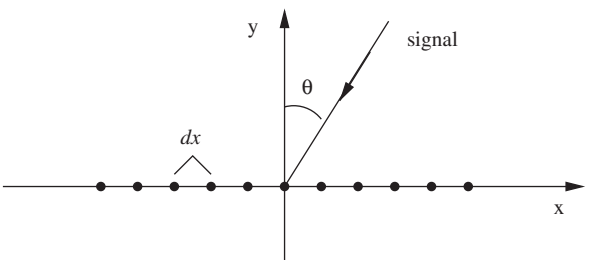

Fig. 1. A uniform linear array.

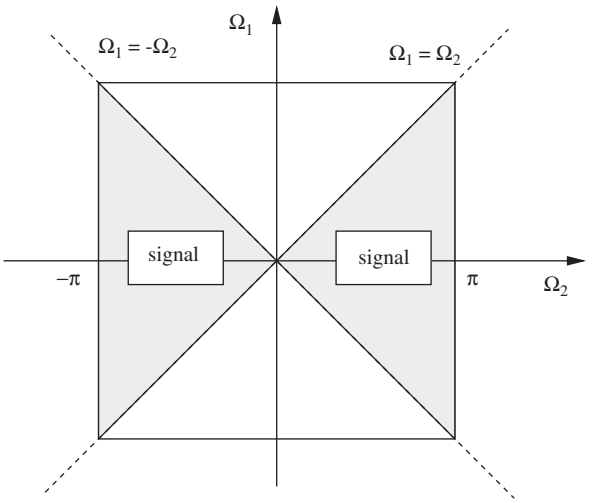

Fig. 2. The possible location of the spatio-temporal spectrum of the impinging signal on the (Ω_1,Ω_2) plane.

$\Omega_1=\Omega\sin\theta$ and $\Omega_2=\Omega$ in (1), we have

$$P(\Omega_1,\Omega_2)=\sum_{m=0}^{M-1}\sum_{n=0}^{J-1} d[m,n]\mathrm{e}^{-\mathrm{j}m\Omega_1}\mathrm{e}^{-\mathrm{j}n\Omega_2}. \tag{2}$$

As the spatio-temporal spectrum of the impinging signal lies on the line $\Omega_1=\Omega_2\sin\theta$, which for a variable angle of arrival θ covers the area between the two lines $\Omega_1=\Omega_2$ and $\Omega_1=-\Omega_2$ on the (Ω_1,Ω_2) plane, as shown in Fig. 2. A method can be developed to obtain a frequency invariant beam pattern by following the design below.

Step 1: Let the desired beam pattern be $F(\sin\theta)$. With the substitution $\sin\theta=\Omega_1/\Omega_2$, for $(\Omega_1,\Omega_2)\in(-\pi;\pi]$ we have

$$P(\Omega_1,\Omega_2)=\begin{cases} F(\Omega_1/\Omega_2), & \left|\dfrac{\Omega_1}{\Omega_2}\right|\leqslant 1\cap\Omega_2\neq 0,\\ A(\Omega_1,\Omega_2) & \text{otherwise,}\end{cases} \tag{3}$$

where $A(\Omega_1,\Omega_2)$ is an arbitrary function to define values for $P(\Omega_1,\Omega_2)$ for the area where a beam pattern does not exist according to Fig. 2. Note that $P(\Omega_1,\Omega_2)$ is a function with a period of 2π.

Step 2: Applying a 2-D inverse Fourier transform to $P(\Omega_1,\Omega_2)$ results in an infinite support of $d[m,n]$. It is difficult to obtain the result analytically; therefore we can apply the 2-D inverse discrete Fourier transform (DFT) as an approximation by sampling $P(\Omega_1,\Omega_2)$ on the (Ω_1,Ω_2) plane in the range of $(-\pi;\pi]$. After applying an inverse DFT to the sampled 2-D values, the resulting $d[m,n]$ needs to be delayed and truncated according to the number of sensors and the FIR filter length.

3. Problem with off-broadside main beam design and its solution

Based on the above design method, we can design an FIB with its main beam in an arbitrary direction. However, although the design result for a broadside main beam is very good, for the design with an off-broadside main

beam, given the same number of array sensors and attached FIR coefficients, it is not as good as the broadside main beam case. Here we give two design examples for a uniform linear array with 16 sensors and an FIR filter length of 20. One is for a broadside main beam and one is for an off-broadside main beam pointing to the direction $\theta = -30^\circ$. The desired ideal response for the broadside main beam example is given by

$$F_1(\sin\theta) = \frac{1}{5}\sum_{m=-2}^{2} \mathrm{e}^{-\mathrm{j}m\pi\sin\theta} \tag{4}$$

and for the off-broadside case it is

$$F_2(\sin\theta) = \frac{1}{5}\sum_{m=-2}^{2} \mathrm{e}^{-\mathrm{j}m\pi(\sin\theta-\sin\pi/6)}. \tag{5}$$

Both designs are obtained by sampling the pattern $P(\Omega_1, \Omega_2)$ by 32×32 points and then truncating the IDFT results to the required dimension of 16×20. The resultant beam pattern for the broadside main beam is shown in Fig. 3, which has a very good frequency invariant property for about $\Omega > 0.3\pi$.

The example for the off-broadside main beam is shown in Fig. 4 and the variation of the response over different frequencies is clearly visible. This problem can be explained by the considerable discontinuity of the periodic function $P(\Omega_1, \Omega_2)$ at $\Omega_2 = \ldots, -3\pi, -\pi, \pi, 3\pi, \ldots$, when the main beam is not pointing to the broadside, as shown in Figs. 5 and 6. Because of the discontinuity incurred when sampling $P(\Omega_1, \Omega_2)$ and subsequently applying the inverse DFT, the response of $P(\Omega_1, \Omega_2)$ around this area cannot be controlled well. This leads to a poor performance of the proposed method, especially for frequencies close to π. This problem also occurs, although less pronounced, even if the main beam is at broadside but the beam pattern is non-symmetric with respect to it.

Since the problem with the off-broadside main design is due to the considerable discontinuity of the periodic function $P(\Omega_1, \Omega_2)$ at $\Omega_2 = \ldots, -3\pi, -\pi, \pi, 3\pi, \ldots$, we can sample the function $P(\Omega_1, \Omega_2)$ in the Ω_2 direction more densely and then permit more coefficients for the corresponding temporal dimension of the beamformer after truncation. For simplicity, we can sample $P(\Omega_1, \Omega_2)$ by a large number in both the directions of Ω_1 and Ω_2. After the inverse DFT, we can truncate the results with a rectangular window and leave much more coefficients in the temporal dimension (FIR filter length) than in the spatial dimension (sensor number). In the example shown in Fig. 7, we sampled $P(\Omega_1, \Omega_2)$ by 256×256 points and then truncated the IDFT results to 16×128. Comparing this result with Fig. 4, we can clearly see the significantly improved frequency invariant property.

Although a better frequency invariant property can be achieved by the proposed approach, the resultant computational complexity for implementing this FIB also increases significantly. For example, the number of coefficients for the off-broadside example in Fig. 4 is only $16 \times 20 = 320$, while for the example in Fig. 7, it is $16 \times 128 = 2048$. In general, the number of real multiplications required for implementing the fullband beamformer is given by

$$C_{full}^{real} = MJ \tag{6}$$

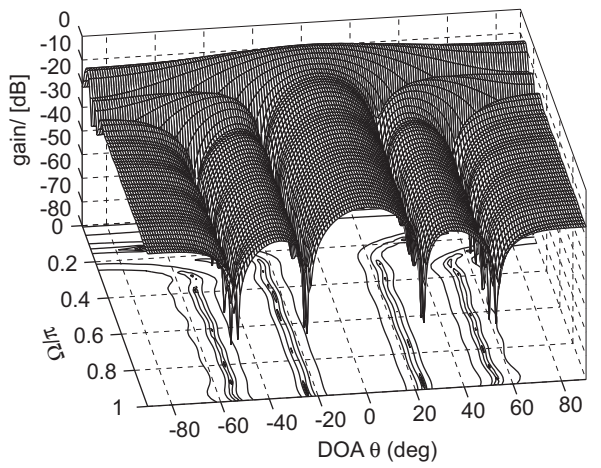

Fig. 3. The designed beam pattern for the linear array with a broadside main beam.

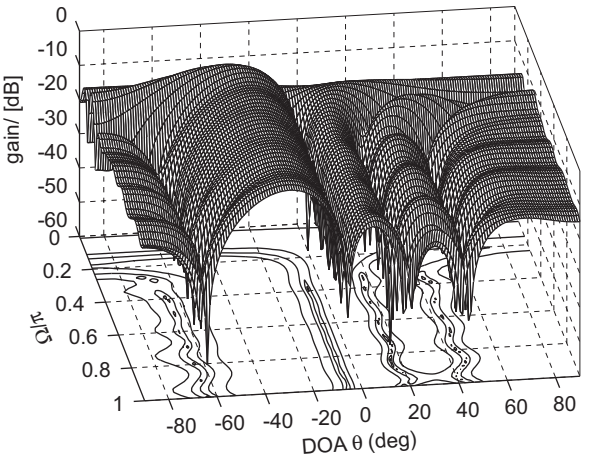

Fig. 4. The designed beam pattern of a linear array with its main beam at $\theta = -30^\circ$.

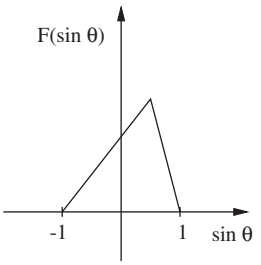

Fig. 5. A desired frequency invariant beam pattern with an off-broadside main beam.

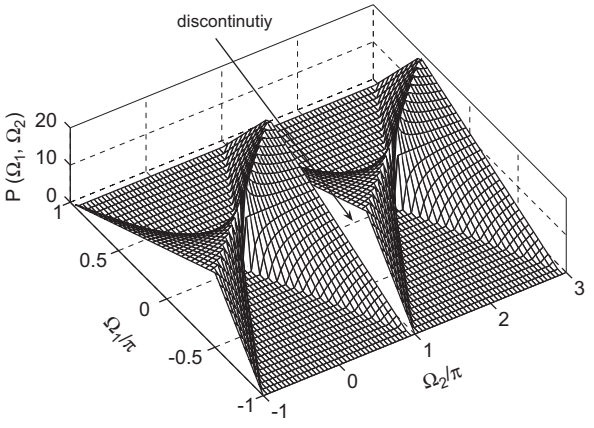

Fig. 6. The discontinuity of $P(\Omega_1,\Omega_2)=F(\Omega_1/\Omega_2)$ when the desired main beam is off-broadside as shown in Fig. 5.

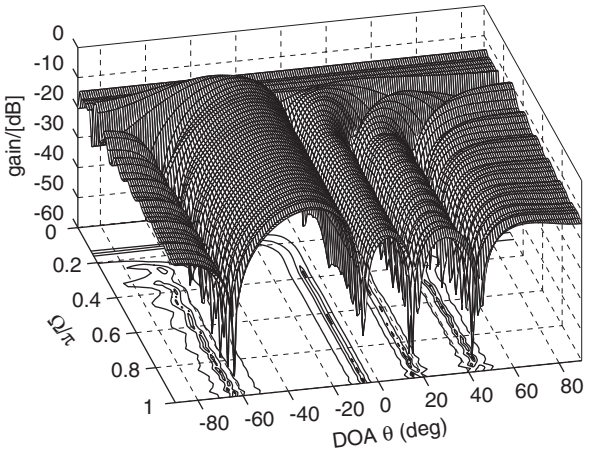

Fig. 7. The design example with an off-broadside main beam in the direction -30° obtained by the proposed method.

for a real-valued input signal and

$$C_{full}^{complex}=2MJ \tag{7}$$

for a complex-valued input signal.

In addition to the above direct approach, another solution to the problem is to design a broadside main beam first, and then steer the array to the desired direction by means of appropriate delays implemented by either some analogue devices or FIR/IIR filters. In this way, the broadside main beam is shifted to the desired direction. However, for the sidelobe region, it is not a simple shift relationship and the response could be very different from the original one [14]. Moreover, the total number of coefficients is still very large taking into account both the steering filters and the original FIR filters of the broadside beamformer.

In the next section, we will implement the proposed FIB in subbands with the aim of reducing its computational complexity and also extending its frequency invariant property over a wider bandwidth.

4. Subband implementations of FIBs

4.1. The first implementation

4.1.1. The subband FIB structure

Fig. 8 shows the general structure of a K-channel filter bank with a decimation factor N, where the input signal $x[n]$ is decomposed into K subbands by an analysis filter bank and each subband signal is then decimated by a factor of $N\leqslant K$. After upsampling, these subbands are recombined by a synthesis filter bank to yield the fullband output signal $\hat{x}[n]$.

For the subband implementation of the FIB based on the uniform linear array, each of the received array signals $x_m[n]$, $m=0,1,\ldots,M-1$, is split into K subbands by the analysis filter bank and the corresponding subband signals form K sets of subband arrays. An FIB is operated in each of the subband arrays and the processed subband signals are then combined together by a synthesis filter bank into the fullband output. There are in total K subband FIBs and each has M subband sensor inputs and its FIR filter length is J_{sub}. Fig. 9 shows this implementation, where the blocks labelled "A" are the analysis filter banks and the block labelled "S" is the synthesis filter bank.

The advantage of this subband implementation is similar to the subband implementation of adaptive filters [15–17], which can be explained by the fact that N subband FIBs are trying to model the original fullband beamformer to have the same spatio-temporal filtering effect. Therefore, due to the subband decomposition and decimation, the FIR filter length J_{sub} of the subband FIBs can be shorter than the original fullband beamformer to achieve a similar performance, in accordance with the sampling rate reduction by a factor of $N\leqslant K$. J_{sub} should not be determined only by the decimation rate N, but also an offset term introduced by transients caused by the filter banks, as in the case of subband adaptive filtering [15,16]. More precisely, we normally choose

$$J_{sub}=\frac{J+l_p}{N}, \tag{8}$$

where l_p is the offset term and is chosen as the length of the prototype filter for the oversampled generalised DFT (GDFT) filter banks [16], which will be used in our subband implementations.

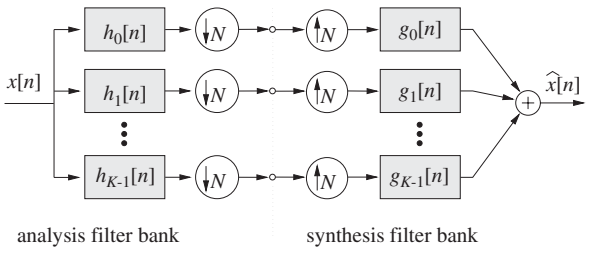

Fig. 8. A general structure of a K-channel filter bank with a decimation factor of N.

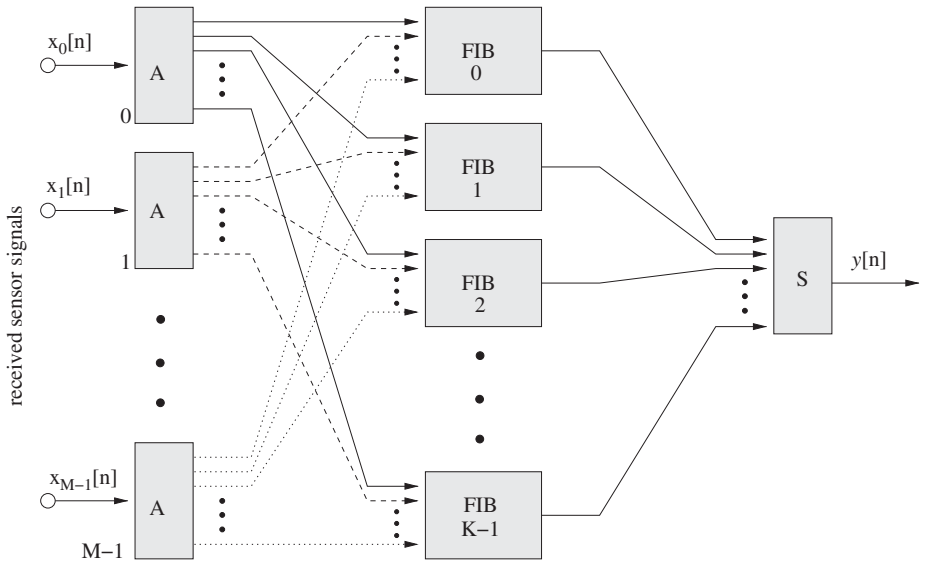

Fig. 9. Subband implementation of the frequency invariant beamformer.

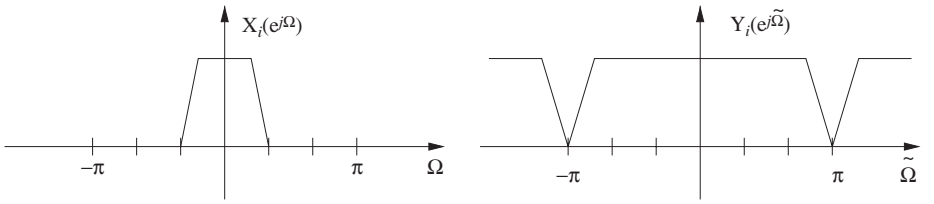

Fig. 10. The spectrum changes after a signal with a bandwidth of $2\pi/3$ is decimated by a factor of $K=3$.

Since the subband FIBs have a shorter length and operate at a lower rate, the computational complexity of the whole system can be much lower than the fullband implementation, when the FIR filters for the fullband beamformer are sufficiently long to render the additional filter bank operations negligible.

4.1.2. Design of subband FIBs

For the design of the subband beamformer, because the normalised signal angular frequency $\tilde{\Omega}$ in decimated subbands has changed after decimation, we need to modify the method in Section 2 to fit the new scenario.

For the design of the i-th subband beamformer, at first, we need to find the relationship $\tilde{\Omega}=S_i(\Omega)$ between the decimated subband $\tilde{\Omega}$ and the fullband Ω. Suppose the spectrum of the output signal of the analysis filter bank is $X_i(\mathrm{e}^{\mathrm{j}\Omega})$ before decimation, then the output spectrum $Y_i(\mathrm{e}^{\mathrm{j}\tilde{\Omega}})$ after decimation is given by [18]

$$Y_i(\mathrm{e}^{\mathrm{j}\tilde{\Omega}})=\frac{1}{K}\sum_{k=0}^{K-1}X_i(\mathrm{e}^{\mathrm{j}((\tilde{\Omega}-2k\pi)/K)}). \tag{9}$$

We can find each $\tilde{\Omega}=S_i(\Omega)$ according to this equation.

For the i-th subband beamformer, its response to the decimated subband input signal can be written as

$$\tilde{P}_i(\tilde{\Omega},\theta)=\sum_{m,n=0,0}^{M-1J_{sub}-1}d_i[m,n]\mathrm{e}^{-\mathrm{j}m\Omega\sin\theta}\mathrm{e}^{-\mathrm{j}n\tilde{\Omega}}, \tag{10}$$

where $d_i[m,n]$ is the coefficients of the i-th subband beamformer. We use the same phase difference $\mathrm{e}^{-\mathrm{j}\Omega\sin\theta}$ between adjacent subband sensor signals as that of the fullband beamformer in (1), because it does not change after decimation. For its response to the original fullband input signal, we have

$$\tilde{P}_i(S_i(\Omega),\theta)=\sum_{m,n=0,0}^{M-1J_{sub}-1}d_i[m,n]\mathrm{e}^{-\mathrm{j}m\Omega\sin\theta}\mathrm{e}^{-\mathrm{j}nS_i(\Omega)}. \tag{11}$$

By substituting $\Omega_1=\Omega\sin\theta$ and $\tilde{\Omega}_2=\tilde{\Omega}$ into (10), we have

$$\tilde{P}_i(\Omega_1,\tilde{\Omega}_2)=\sum_{m,n=0,0}^{M-1J_{sub}-1}d_i[m,n]\mathrm{e}^{-\mathrm{j}m\Omega_1}\mathrm{e}^{-\mathrm{j}n\tilde{\Omega}_2}. \tag{12}$$

Thus, we can obtain $d_i[m,n]$ by applying the inverse Fourier transform to the desired subband response $\tilde{P}_i(\Omega_1,\tilde{\Omega}_2)$. As $\tilde{\Omega}=S_i(\Omega)$ and $\Omega_2=\Omega$, we also have $\tilde{\Omega}_2=S_i(\Omega_2)$, then

$$\tilde{P}_i(\Omega_1,S_i(\Omega_2))=P(\Omega_1,\Omega_2) \tag{13}$$

for the i-th subband.

From the discussion above, we obtain a modified method applicable to the subband FIB design.

We first obtain $P(\Omega_1,\Omega_2)$ from the fullband beamformer design method. Then we uniformly sample Ω_1 and $\tilde{\Omega}_2$ in $(-\pi;\pi]$ with $M_{\max}\times J_{\max}$ points, where $M_{\max}\geqslant M$ and $J_{\max}\geqslant J_{sub}$. We calculate $\tilde{P}_i(\Omega_1,\tilde{\Omega}_2)$ on these points

according to (13). Applying the inverse DFT to the result, we then obtain $d_i[m,n]$ with a dimension $M_{\max} \times J_{\max}$, which needs to be truncated to fit the subband FIB dimension $M \times J_{sub}$.

However, there is one problem when calculating $\tilde{P}_i(\Omega_1, \tilde{\Omega}_2)$ according to (13), as one value of $\tilde{\Omega}_2 = \tilde{\Omega} = S_i(\Omega_2)$ in general corresponds to K different values of $\Omega_2 = \Omega$ according to (9). To remove this ambiguity, the bandwidth of each subband signal before decimation should be limited to no more than $2\pi/N$ (including both the negative and positive frequencies). Fig. 10 shows the spectrum changes after a signal with a bandwidth $2\pi/3$ is decimated by a factor $N = 3$. Thus, although one value of $\tilde{\Omega}_2$ ($\tilde{\Omega}$) still corresponds to several different values of Ω_2 (Ω), which is determined by (9) and cannot be changed, only on one value of Ω_2 (Ω), the subband signal before decimation is non-zero and on all the other values of Ω_2 (Ω), the subband signal is zero. We will then use that value to calculate the unique $\tilde{P}_i(\Omega_1, \tilde{\Omega}_2)$ according to (13). In the example of Fig. 10, the point $\tilde{\Omega} = 2\pi/3$ corresponds three different values of Ω, which are, respectively, $\Omega = -4\pi/9, 2\pi/9$ and $8\pi/9$. As $X_i(e^{j\Omega}) = 0$ for $\Omega = -4\pi/9$ and $8\pi/9$, we will choose $\Omega = 2\pi/9$ as the corresponding point of $\tilde{\Omega} = 2\pi/3$.

4.1.3. Computational complexity

With this bandwidth constraint, we cannot use the perfect-reconstruction maximally decimated ($N = K$) filter banks in our subband beamformer design, as the bandwidth of the analysis filter bank in such systems is always larger than $2\pi/N$. As a result, we have to employ the oversampled ($N > K$) filter banks with a very low aliasing level, such as the oversampled GDFT filter banks [19]. In such filter banks, the analysis filters are derived from a real-valued lowpass prototype FIR filter $p[n]$ of length l_p by a GDFT according to

$$h_k[n] = e^{j(2\pi/K)(k+k_0)(n+n_0)} p[n] \quad \text{with } k = 0, \ldots, K-1 \text{ and } n = 0, \ldots, l_p - 1, \tag{14}$$

where k_0 and n_0 are offset terms introduced into the frequency and time indices of the DFT. Specifically, in conjunction with $k_0 = \frac{1}{2}$, for a real-valued input signal $x[n]$ it is sufficient to only process the first $K/2$ subbands covering the frequency interval $[0; \pi]$ as the remaining subbands are the complex conjugate versions of these subbands.

The modulation approach allows for both low memory consumption for storing filter coefficients and an efficient polyphase implementation. According to [20], the number of real multiplications required to implement the GDFT filter bank (analysis or synthesis) is

$$C_{GDFT}^{real} = \frac{1}{N}(l_p + 4K \log_2 K + 4K) \tag{15}$$

for a real-valued input signal and

$$C_{GDFT}^{complex} = \frac{1}{N}(2l_p + 4K \log_2 K + 8K) \tag{16}$$

for a complex-valued input signal. Note the term $4K \log_2 K$ in the above two equations is derived from the computational complexity when we implement the oversampled GDFT filter banks using fast Fourier transforms (FFTs) based on K being a power of two. For other values of K, a similar result can be obtained and Eqs. (15) and (16) are for guidance only.

For each of the subband beamformers, the number of multiplications required is $4MJ_{sub} = 4M(J + l_p)/N$ (for the GDFT filter banks, the input to the subband FIBs is complex-valued and each of the subband FIBs is also complex-valued). There are in total M analysis filter banks and one synthesis filter bank and the signal rate for subband FIBs is $1/N$ of the fullband one. Therefore the total number of multiplications for the whole subband FIB system shown in Fig. 9 is

$$C_{sub}^{real} = \frac{M+1}{N}(l_p + 4K \log_2 K + 4K) + \frac{2KM(J + l_p)}{N^2} \tag{17}$$

for a real-valued input signal and

$$C_{sub}^{complex} = \frac{M+1}{N}(2l_p + 4K \log_2 K + 8K) + \frac{4KM(J + l_p)}{N^2} \tag{18}$$

for a complex-valued input signal.

As an example, the number of multiplications $C_{sub}^{complex}$ and $C_{full}^{complex}$ as a function of the fullband FIR filter length J is shown in Fig. 11 for the case with $M = 16, K = 10, N = 8$, and $lp = 110$. The dashed line is for the subband FIB and the dotted line is for the fullband FIB. For $J \leqslant 91$, the computational complexity of the subband FIB is always higher than that of the fullband one; when $J > 91$, we start to have savings with the subband FIB and the larger the fullband FIR filter length J, the more savings we have in computational complexity.

4.2. The second implementation—scaled aperture

The spatial resolution of a beamformer is reciprocally proportional to both the aperture of the sensor array and the frequency of the impinging signal. Therefore, it is difficult to achieve a constant beamwidth for lower frequencies. To extend the constant beamwidth property to a frequency as low as possible, we here propose the FIB with a scaled aperture, which is shown in Fig. 12, depicting the exemplary case for $M = 4$ sensors for each

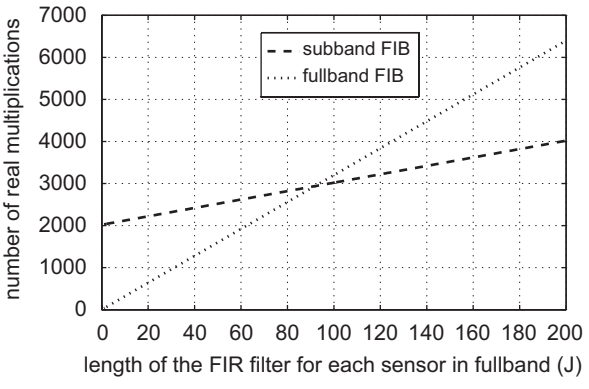

Fig. 11. A comparison of the computational complexity between the fullband FIB and its subband implementation.

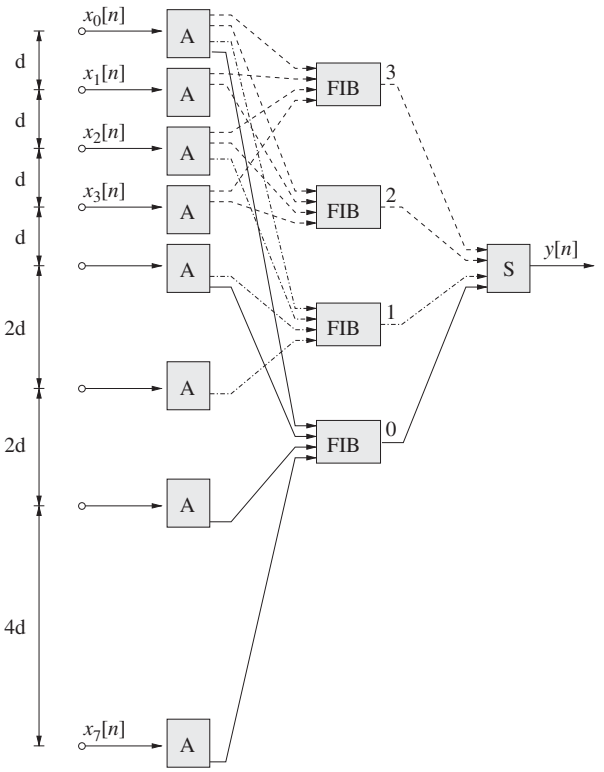

Fig. 12. Proposed beamforming structure with scaled array aperture for FIBs in various octave bands.

octave and beamformers operating in four uniformly split decimated subbands, with each having a bandwidth $\pi/4$, whereby the array signals are drawn from a total of eight nested sensors. For the three octave groups of subband FIBs, FIB #0 operates on the lowest band, FIB #1 forms the second octave, and the remaining two FIBs are responsible for the highest octave band covered by two subbands. As indicated in Fig. 12, not all subbands are required for processing from each sensor.

As the array spacing is different for each octave of subband beamformers, we need to change the subband beamformer design procedure correspondingly. In Fig. 12, beamformers 3 and 2 have a standard spacing of $d=\lambda_{\min}/2$, so we can apply the previous design procedure directly; for beamformers 1 and 0, they have a spacing of $\lambda_{\min}$ and $2\lambda_{\min}$, respectively, then we must consider this difference in our design. Suppose the spacing of the subband beamformer is σ times the standard spacing $\lambda_{\min}/2$, then its response to the original fullband input signal is

$$\tilde{P}_i(S_i(\Omega),\theta)=\sum_{m,n=0,0}^{M_iJ_i} d_i[m,n]\mathrm{e}^{-\mathrm{j}m\sigma\Omega\sin\theta}\mathrm{e}^{-\mathrm{j}nS_i(\Omega)}, \tag{19}$$

where $d_i[m,n]$ is the coefficients of the i-th subband beamformer with a dimension of $M_i\times J_i$. By substituting $\tilde{\Omega}_1=\sigma\Omega\sin\theta=\sigma\Omega_1$ and $\tilde{\Omega}_2=S_i(\Omega)$ into (19), we have

$$\tilde{P}_i(\tilde{\Omega}_1,\tilde{\Omega}_2)=\sum_{m,n=0,0}^{M_iJ_i} d_i[m,n]\mathrm{e}^{-\mathrm{j}m\tilde{\Omega}_1}\mathrm{e}^{-\mathrm{j}n\tilde{\Omega}_2}. \tag{20}$$

The relationship between the subband beamformer response and the fullband beamformer response is given by

$$\tilde{P}_i(\sigma\Omega_1,S_i(\Omega_2))=P(\Omega_1,\Omega_2). \tag{21}$$

Then the design can be modified as follows.

First, we uniformly sample $\tilde{\Omega}_1$ and $\tilde{\Omega}_2$ in $(-\pi;\pi]$ with $M_{\max}\times J_{\max}$ points. Then we obtain the response $\tilde{P}_i(\tilde{\Omega}_1,\tilde{\Omega}_2)$ on these points according to (21). With the inverse DFT, the temporal response $d_i[m,n]$ with a dimension $M_{\max}\times J_{\max}$ is obtained and then truncated to the dimension $M_i\times J_i$.

4.3. Design examples

We give one example for each of the implementations. Both are based on the same desired ideal response with a main beam pointing to the direction $\theta=-30^\circ$, as given in (5) of Section 3.

For the first one, we employ the $K=10$-channel oversampled GDFT filter banks with a decimation ratio $N=8$. The length of the prototype filter is $l_p=110$. Each of the received sensor signals is split into 10 subbands and in total there are 10 subband beamformers, each of which has a dimension of 12×29 since $J_{sub}=(128+110)/8\approx 29$. The resultant beam pattern is shown in Fig. 13, which is very similar to the example given in Fig. 7, except for the frequencies very close to $\Omega=\pi$. For its response at $\Omega=\pi$, it seems that the discontinuity problem has become more serious in subbands. However, this problem can be avoided easily since it is only limited to frequencies extremely close to π and has no obvious effect on other frequencies. Suppose the maximum frequency of interest is $\omega_{\max}$. When we design this broadband array, we can consider its operating frequency to be $\omega_{\max}+\delta$, where $\delta>0$ is a very small value. In this way, $\omega_{\max}+\delta$ will correspond to the normalised frequency $\Omega=\pi$ and $\omega_{\max}$ corresponds to the normalised frequency a little lower than $\Omega=\pi$. Thus, the resultant array can maintain a satisfactory frequency invariant response over the bandwidth of interest below $\omega_{\max}$.

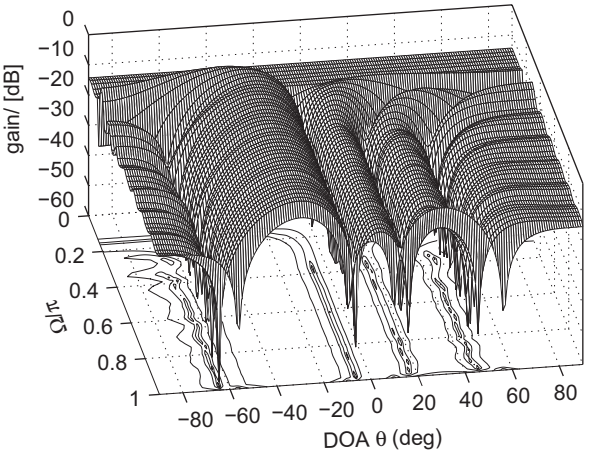

Fig. 13. The resultant beam pattern for the uniformly spaced subband linear array.

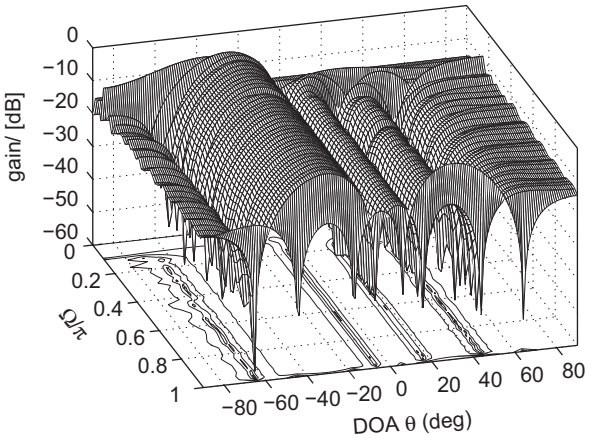

Fig. 14. The resultant beam pattern for the scaled aperture array.

For the computational complexity of this subband FIB system, for a real-valued input signal, it is $C_{sub}^{real} = 1761$ and for the corresponding fullband FIB, it is $C_{full}^{real} = 2048$; for the complex-valued case, we have $C_{sub}^{complex} = 3320$ and $C_{full}^{complex} = 4096$. In both cases, a much lower computational complexity has been achieved by the subband-based beamformer.

Next, for the array with scaled apertures, we employ the same oversampled GDFT filter banks. There are two octaves. The first two channels and the last two channels belong to the first octave; the six channels in the middle belong to the second octave. For each of them, the subband beamformer has a dimension of 16×29. There are 16 sensors for each octave and in total there are $16 + 8 = 24$ sensors. As a result, we have in total 24 analysis filter banks and one synthesis filter bank, i.e. eight more filter banks than the first example. The number of subband FIBs is the same as the first one. Then the total number of real multiplications for this implementation is $C_{scaled}^{real} = 1761 + 8 \times C_{GDFT}^{real} = 2044$ for real-valued input signals and $C_{scaled}^{complex} = 3320 + 8 \times C_{GDFT}^{complex} = 3753$ for complex-valued input signals. So, although this scaled aperture system has a higher complexity than the first subband implementation, it is still lower than the fullband one and its frequency invariant property has been extended to as low as $\Omega = 0.1\pi$, as shown in Fig. 14.

5. Conclusions

We have studied the off-broadside main beam design problem for FIBs and one solution was proposed by increasing the temporal dimension of the beamformer in combination with a denser sampling in the Fourier domain, where a desired response is to be matched. The resultant beamformer has a much higher computational complexity and to reduce this complexity and also improve its frequency invariant property at lower frequencies, two subband implementations are proposed. In the first structure, the received array signals are split into sets of subbands and an FIB is operated in each set of the decimated subbands. It has a much lower computational complexity compared to the fullband implementation. In a refinement to the first structure, we change the sensor spacings of different subband signals, leading to a class of FIBs with scaled apertures with improved frequency invariant property at lower frequencies. To remove the spectrum ambiguity of the design process, oversampled filter banks are employed in the subband decomposition, instead of the maximally decimated ones. Design examples have been provided to show the effectiveness of the two subband implementations.

References

[1] H.L. Van Trees, Optimum Array Processing, Part IV of Detection, Estimation, and Modulation Theory, Wiley, New York, USA, 2002.
[2] D.P. Scholnik, J.O. Coleman, Formulating wideband array-pattern optimizations, in: Proceedings of the IEEE International Conference on Phased Array Systems and Technology, Dana Point, CA, May 2000, pp. 489–492.
[3] S.F. Yan, Y.L. Ma, Design of FIR beamformer with frequency invariant patterns via jointly optimizing spatial and frequency responses, in: Proceedings of the IEEE International Conference on Acoustics, Speech, and Signal Processing, Philadelphia, USA, March 2005, pp. 789–792.
[4] H. Duan, B.P. Ng, C.M. See, J. Fang, Applications of the SRV constraint in broadband pattern synthesis, Signal Processing 88 (April 2008) 1035–1045.
[5] Y. Zhao, W. Liu, R.J. Langley, Efficient design of frequency invariant beamformers with sensor delay-lines, in: Proceedings of the IEEE Workshop on Sensor Array and Multichannel Signal Processing, Darmstadt, Germany, July 2008, pp. 335–339.
[6] D.B. Ward, R.A. Kennedy, R.C. Williamson, Theory and design of broadband sensor arrays with frequency invariant far-field beam patterns, Journal of the Acoustic Society of America 97 (2) (February 1995) 1023–1034.
[7] T. Sekiguchi, Y. Karasawa, Wideband beamspace adaptive array utilizing FIR fan filters for multibeam forming, IEEE Transactions on Signal Processing 48 (1) (January 2000) 277–284.
[8] W. Liu, S. Weiss, J.G. McWhirter, I.K. Proudler, Frequency invariant beamforming for two-dimensional and three-dimensional arrays, Signal Processing 87 (November 2007) 2535–2543.
[9] W. Liu, S. Weiss, Design of frequency invariant beamformers for broadband arrays, IEEE Transactions on Signal Processing 56 (2) (February 2008) 855–860.
[10] Y.M. Zhang, K.H. Yang, M.G. Amin, Adaptive array processing for multipath fading mitigation via exploitation of filter banks, IEEE Transactions on Antennas and Propagation 49 (4) (April 2001) 505–516.
[11] W.H. Neo, B. Farhang-Boroujeny, Robust microphone arrays using subband adaptive filters, IEE Proceedings—Vision, Image and Signal Processing 149 (1) (February 2002) 17–25.
[12] W. Liu, S. Weiss, L. Hanzo, A subband-selective broadband GSC with cosine-modulated blocking matrix, IEEE Transactions on Antennas and Propagation 52 (March 2004) 813–820.
[13] Y.M. Zhang, K.H. Yang, M.G. Amin, Subband array implementations for space–time adaptive processing, EURASIP Journal on Applied Signal Processing 2005 (4) (January 2005) 99–111.
[14] W. Liu, S. Weiss, Off-broadside main beam design for frequency invariant beamformers, in: Proceedings of the International ITG/IEEE Workshop on Smart Antennas, Darmstadt, Germany, February 2008, pp. 190–194.
[15] A. Gilloire, M. Vetterli, Adaptive filtering in subbands with critical sampling: analysis, experiments and applications to acoustic echo cancelation, IEEE Transactions on Signal Processing SP-40 (8) (August 1992) 1862–1875.
[16] S. Weiss, R.W. Stewart, On Adaptive Filtering in Oversampled Subbands, Shaker Verlag, Aachen, Germany, 1998.
[17] M.R. Petraglia, R.G. Alves, P.S.R. Diniz, New structures for adaptive filtering in subbands with critical sampling, IEEE Transactions on Signal Processing 48 (12) (December 2000) 3316–3327.
[18] P.P. Vaidyanathan, Multirate Systems and Filter Banks, Prentice-Hall, Englewood Cliffs, NJ, 1993.
[19] R.E. Crochiere, L.R. Rabiner, Multirate Digital Signal Processing, Prentice-Hall, Englewood Cliffs, NJ, 1983.
[20] S. Weiss, R.W. Stewart, Fast implementation of oversampled modulated filter banks, IEE Electronics Letters 36 (17) (August 2000) 1502–1503.